1

COMPUTATIONAL MODELS FOR DISORDERED NANOWIRE NETWORKS AND THEIR APPLICATION

MOTIVATION

The conductance of a nanowire network (NWN) depends on a multitude of underlying parameters; the length and diameter distributions of nanowires[1–5], inter-wire junction resistances[6], resistance of nanowire segments[7], wire density[8], and electrode shape[9]. All of these parameters combine to give a unique connectivity profile for each NWN which determines its conductance. A common method of numerically solving this percolative transport problem[10] is to map the NWN onto a node-voltage graphical representation where each nanowire is a node in the graph and is connected to its nearest neighbours by a resistor corresponding to the inter-wire junction. Kirchhoff's current laws and Ohm's law are applied to the node-voltage graph to calculate the conductance[11]. An implicit assumption is being made in this approach, that the junction resistance is much higher than the nanowire resistance and so dominate the electrical properties of the network. This approach shall be referred to as the Junction Dominated Assumption (JDA) henceforth.

Monte Carlo simulations of conductive stick networks show that their electrical properties are highly sensitive to the ratio R_{in}/R_j[4,7,14] where R_j is the resistance of a junction and R_{in} is that of a wire segment. The JDA model has successfully calculated the resistive properties of carbon nanotube networks as the nanotube resistance is negligible compared with the resistance of a nanotube junction[1,12]. Metallic nanowire junctions however have been shown to have a relatively low resistance[13] and as a result the nanowires themselves have a sizeable impact on network conduc-

tivity. With the demand for increasing NWN conductivity for optoelectric device applications, R_j is continuously being minimised by effective annealing techniques and so a replacement for the irrelevant JDA is needed for these systems. In this chapter we introduce a model that includes nanowire resistances, the Multi-Nodal Representation (MNR) model, and show how both MNR and JDA models depend differently on the underlying parameters mentioned at the start of the chapter.

A fundamental issue with nanowire network simulations is the inherent spatial randomness of wire positions and their impact on network connectivity. Experimental measurements can only be related to the average results of simulations with matching underlying parameters in order to obtain meaningful results[6]. This approach however fails to give a complete understanding of the electrical properties of a unique NWN, merely an understanding of how it compares to the average. To directly compare computational simulation with experimental measurements we developed a method to digitally capture the positions and orientations of nanowires from Scanning-Electron-Microscope images of NWNs. This approach allows calculated sheet resistances to be compared directly with experimentally measured sheet resistances, removing geometrical randomness from the comparison. The goal of this chapter is to compare MNR and JDA simulations using both configurational averaging and digitised networks with experimental samples to understand the effect of nanowire resistance on certain network properties.

The layout of this chapter is as follows. In section 1.2 The JDA and MNR models are presented and the computational simulations are outlined. In sections 1.3 & 1.4 MNR and JDA are applied to simulations of NWNs and the effect of the various parameters of the NWNs are explored. The dependence of MNR on the nanowire resistances and the effect of the junction resistance in both models are presented in section 1.3. The dependence of wire densities and wire lengths are determined through spatial configurational averaged simulations in section 1.4. In section 1.5 images of experimental NWNs are processed and the JDA and MNR are applied to the digitised network. The digitised network can be used to approximate the

junction resistance of the samples and these approximations were compared with a distribution of junction resistances that were experimentally measured by Bellew et al[13]. The ultimate conductivity of a NWN, that which is obtained when junctions are annealed to perfect conductors, is calculated for each of the experimental samples. A dimensionless parameter that illustrates the potential for network conductance improvement is introduced and its dependence on several network parameters are presented. There is a short chapter summary in section 1.6.

GRAPHICAL REPRESENTATIONS OF NANOWIRE NETWORKS

To calculate the global resistive properties of the NWN it must be mapped into a node voltage graph, essentially capturing the connectivity information of a NWN in a mathematical graph so that Kirchhoff's matrix equations introduced in chapter 2 can be used. In the JDA mapping each wire is represented by a circuit node at a common voltage connected to other wires by a certain number of junction resistors determined by its connectivity within the network. A NWN with N_w wires will result in a resistive graph with N_w nodes. An off-diagonal element of the Kirchhoff matrix (K_{ij}^{jda}) is the conductance of the inter-wire junction between wires i and j, the conductance is zero if there is no junction between the wires. Figure 1.1(a) is a sketch of a simple NWN (top) with its JDA graphical representation (bottom). There there are three nodes in the graphical representation, one for each nanowire, and two inter-wire junctions a resistance R_j. Note that there is no junction between wires W_1 and W_2, thus there is no resistor in the graphical representation. The locations of the nanowires are irrelevant in the JDA, it is only the connectivity profile of the network that determines the electrical properties. As this mapping only acts on the inter-wire connectivity the electrical properties of the nanowire segments are entirely omitted from this model.

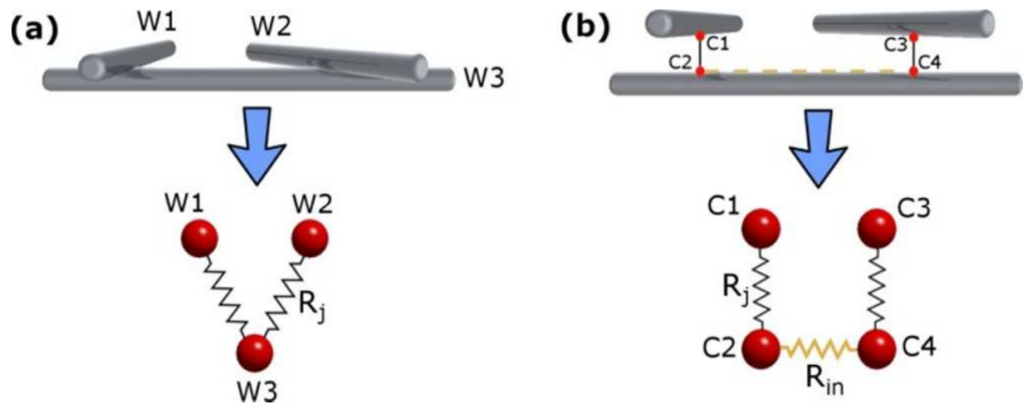

Figure 1.1: a) A sketch of a simple NWN with 3 wires labelled W_i $i = 1, 2, 3$ and two inter-wire junctions, one between wires W_1 and W_2 and another between wires W_1 and W_3. Underneath the sketch is a graphical representation of the NWN, there are three nodes corresponding to the three wires and two inter-wire junction resistors represented by black resistors and labelled R_j. b) An expanded view sketch of a simple NWN with 3 wires with two inter-wire junctions. The 4 connection nodes, two for each inter-wire junction, are shown as the red dots labelled C_i, $i = 1, 2, 3, 4$. Underneath the sketch is an MNR graphical representation of the NWN. Connection nodes associated with the same junction are connected by a junction resistor R_j and shown in black. The connection nodes that are adjacent on wire 3, C_2 and C_4 are connected by an nanowire segment resistor R_{in} illustrated by the yellow resistor. Note: Image quality to be updated

While the JDA is suitable for materials with a large junction resistance the nanowire resistance cannot be omitted for materials where it is comparable with that of the junctions. In order to include the inner wire resistances a new voltage-node mapping is needed. Consider a wire that has b intersections with other wires thus partitioning it into $b + 1$ wire sections each with a classical resistance given by

$$R_{in} = \frac{\rho \ell_i}{A_c} \tag{1.2.1}$$

Where ρ is the wire's resistivity, ℓ_i is the length of wire section i and A_c is the cross sectional area of the wire. Note that two of the sections, at either end of the nanowire, play no part in the electrical properties of the network as they in a sense 'dead-ends' for current flow[18]. The inter-wire connection points, which partition

the wire segments, are a natural choice for the nodes in the new node-voltage mapping which we shall call Multi-Nodal Representation (MNR) henceforth. For each inter-wire junction there are two connection nodes, one on each wire, and are connected by a junction resistor. Adjacent connection nodes on the same nanowire are joined with an nanowire resistor. A sketch of a simple NWN and the corresponding MNR graphical representation is presented in Figure 1.1(b). The total number of nodes in this scheme is $2N_j$, where N_j is the total number of junctions in the network. The nanowire resistor between the nodes C_2 and C_4 is depicted in yellow, the two junction resistors are also shown in the graphical representation. Note that the dead-ends are not included in the graphical representation. Unlike the JDA model, the spatial configuration of the wires and their intersections in the network is required in the MNR model as the distances between adjacent connection nodes is needed for the calculation of nanowire resistances. If two nodes share the same (x,y) coordinates then they are associated with the same inter-wire junction and are on different wires.

In chapter 2 the junction density was related to the wire density in a network by $n_j = \alpha L^2 n_w^2$ meaning that the total number of junctions is $N_j = \alpha L^2 N_w^2/B$ where L is the length of each wire, B is the total area of the NWN and α is a constant ≈ 0.318. The Kirchhoff matrix for the JDA model of a network is of size $N_w \times N_w$ representing a system of N_w linear equations. In the MNR model, the Kirchhoff matrix is of size $2N_j \times 2N_j$ representing $2N_j = 2\alpha L^2 N_w^2/B$ linear equations. The computational power to solve a set of $2N_j$ linear equations in the MNR model is an order of magnitude higher than needed for the JDA model, i.e. $O(N_w^2)$ for the MNR versus $O(N_w)$ for the JDA. Herein lies a disadvantage of the MNR model as the required computational power quickly becomes too demanding for networks with many wires.

In both JDA and MNR the computational simulations are performed as follows. A number of nanowires are assigned pseudo-random positions and orientations with their center points confined to a predefined area. Where two wires intersect

with one-another an inter-wire junction occurs, the positions and associated wires of each intersection are recorded. The MNR and JDA mapping can be applied to the NWN with the connectivity profile and the wire positions. The Kirchhoff matrix for both can be formulated and numerically solved to calculate the sheet resistance of the network. The same network can be recreated a number of times by simply choosing the same random number generator seed used to generate the positions and orientations of wires in simulations allowing the impact of particular network parameters to be assessed on a fixed geometry. The two models are an excellent tool to determine the effect of all of the underlying properties on the resulting sheet resistance of the NWN.

The properties of the NWN can be grouped into two main categories, the geometric and the resistive parameters. The geometric parameters are those that effect the actual connectivity of the NWN; the wire density (n_w) and wire length (L). Wire diameters are not used to determine the intersection of two nanowires and so is not included as a geometrical parameter. A change in one of these parameters totally changes the connectivity profile of the NWN and two networks with the same wire lengths and densities can have vastly different sheet resistances due to stochastic fluctuations in wire position and orientation. To combat this Monte Carlo simulations are performed whereby a large number of NWNs are generated for each combination of wire density and wire lengths and so the effect of each parameter can be determined. The resistive parameters do not alter the connectivity profile of the NWN but change the magnitude of the resistors in the network. These are the junction resistance (R_j), the wire resistivity (ρ), and the wire diameter D. The effect of these parameters are best illustrated by fixing a NWN connectivity profile and calculating the change in sheet resistance associated with changes to these parameters. The effect of these two categories of parameters will be explored in the proceeding sections.

IMPACT OF RESISTIVE PARAMETERS ON NANOWIRE NETWORK RESISTANCE

The resistive properties of nanowires do not alter the connectivity of the NWN but they do however change the resistor values in the network. Both JDA and MNR were applied to the same network geometry in order to keep the connectivity profile the same and allow for a direct comparison between models. Figure 1.2 is a visualisation of the simulated network which is of size $20\mu m \times 20\mu m$, $L = \mu m$, and $n_w = 0.4$ NW/μm^{-2}. This network will be the benchmark geometry used to identify the dependence of the sheet resistance (R_s) on ρ, D and R_j in this section.

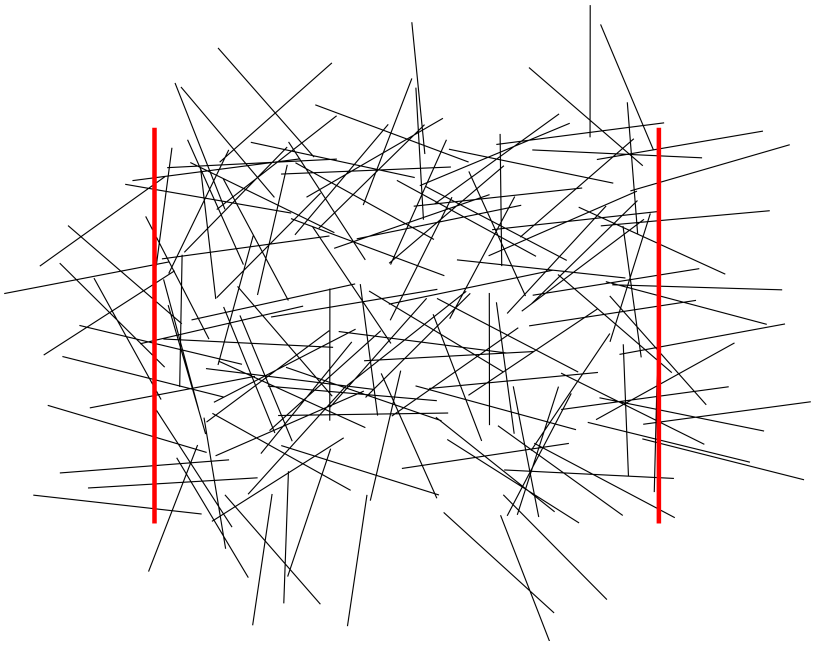

Figure 1.2: A visualisation of a simulated network to be used as a fixed geometry to determine the role of resistive parameters on network conductivity. Wires are 7 μm in length and there is a wire density of 0.4 μm^{-2}. The network has dimensions $20\mu m \times 20\mu m$ and the electrodes are represented by the thick red lines vertical lines either side of the network.

Effect of Junction Resistance on Network Conductance

The common resistive parameter between MNR and JDA is the junction resistance. In this comparison between the models every junction resistance was assigned the same value R_j. The resistivity and wire diameters were fixed in the MNR to values typical of Ag/PVP core-shell nanowires, $\rho = 22.6n\Omega m$ and $D = 50nm$[19]. Figure 1.3 shows the effect of increasing R_j on the calculated sheet resistance for both the MNR and JDA models particular to the network geometry shown in Figure 1.2.

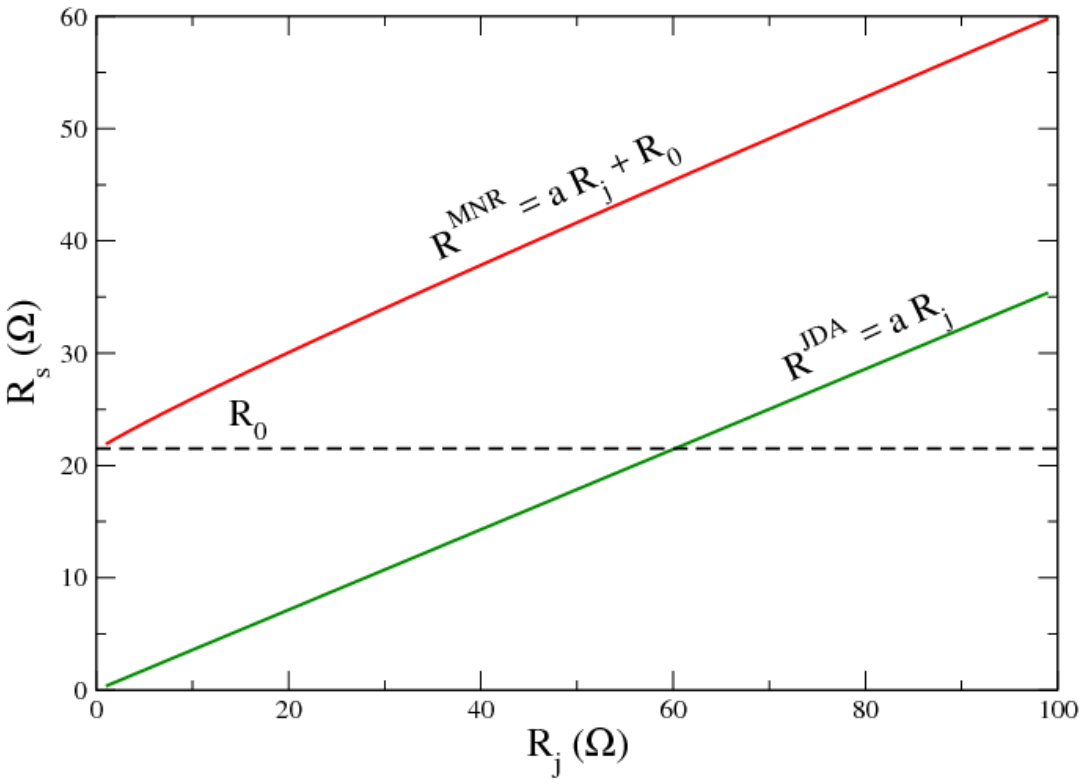

Figure 1.3: The effect of the resistance of each junction in the network on the sheet resistance of the network shown in Fig. 1.2. The sheet resistance R_s depends linearly on the junction resistance for both the MNR and JDA models. In fact the slope of both linear functions (a) is the approximately the same for both functions at $a \approx 0.37$. The effect of the nanowire resistance in the MNR manifests as the addition of a constant R_0 and corresponds to R_s^{MNR} with $R_j = 0$.

A striking feature of Figure 1.3 is that the sheet resistance of the MNR and JDA depends linearly on the junction resistance, both linear relationships having the same slope.

$$R_s^{JDA} = \alpha R_j \tag{1.3.1}$$

$$R_s^{MNR} = \alpha R_j + R_0 \tag{1.3.2}$$

where $\alpha \approx 0.37$ and $R_0 \approx 21\Omega$ in this case. Intuitively the JDA functional form behaves as desired, one expects a sheet resistance of zero if every junction in the network has zero resistance. Similarly the MNR functional behaves as expected, as the junction resistance is brought to zero the sheet resistance tends to the nanowire resistance of the network R_0. The inclusion of the nanowire resistance drastically increases the sheet resistance for a given junction resistance for this NWN. For example, in the MNR model the $R_s = R_0 = 21\Omega$ for $R_j = 0$. In order to achieve this sheet resistance in the JDA the junction resistance required is $R_j = 21/\alpha \approx 60\Omega$. This difference between the required R_j in both models can cause their overestimation when comparing simulations and experiments, this point is discussed further in a later section.

The value of the slope for both models gives an understanding of the nature of current flow through the NWN. A NWN is a mass of parallel paths between the two electrodes, all of varying length. A simple interpretation of current flow through the NWN is that there are P parallel paths of S junction resistors in series. S and P are characteristic parameters unique to each network. The sheet resistance of such a network in the JDA model is

$$R_s = \frac{SR_j}{P} \tag{1.3.3}$$

Comparing this to equation 1.3.1 shows that $\alpha = \frac{S}{P}$. Thus for $\alpha < 1$ we can argue that the current flow through the NWN is through many parallel paths P, more paths than the number of junctions connected in series S. If $\alpha > 1$ then the current

flows through few paths between electrodes. One expects that a depends on the connectivity profile, where highly connected NWNs will have a much lower slope than sparse networks.

A symmetry argument of sorts can be made to explain the linear relationship between R_s and R_j in the JDA. If the only difference between two networks is a constant shift of every resistors value then the resistance between any nodes in the network should shift by the same amount. A mathematical proof of this can also be made by making use of the Kirchhoff Matrix formalism defined in chapter 2. If every resistor in the NWN has the same value R then the Kirchhoff matrix is

$$\hat{K} = \frac{1}{R}\hat{\mathcal{L}} = \Gamma\hat{\mathcal{L}} \tag{1.3.4}$$

recalling that $\hat{\mathcal{L}}$ is the Laplacian matrix defined in chapter 2 and $\Gamma = 1/R$. The Kirchhoff matrix, along with the current vector ($\vec{I}$) which defines the sourced and drained current to the network, is used to solve the potential at each node in the network. Consider the case where $R = 1$, Kirchhoff's system of linear equations are

$$\hat{\mathcal{L}}\vec{V}^{\mathcal{L}} = \vec{I} \tag{1.3.5}$$

where $\vec{V}^{\mathcal{L}}$ is the solution to this equation. The resistance between the source current node (node m) and the drain current node (node n) is

$$R^{\mathcal{L}}_{mn} = \frac{|\vec{V}^{\mathcal{L}}_m - \vec{V}^{\mathcal{L}}_n|}{i_0} \tag{1.3.6}$$

where i_0 is the current flowing between the nodes. Now consider the case where $R \neq 1$ and the current vector is the same as before. We now have

$$\hat{K}\vec{V} = \frac{1}{R}\hat{\mathcal{L}}\vec{V}^k = \vec{I} \tag{1.3.7}$$

Using equation 1.3.5 we can equate $\frac{1}{R}\hat{\mathcal{L}}\vec{V}^{K} = \hat{\mathcal{L}}\vec{V}^{\mathcal{L}}$ and so the solved voltage vectors are related by

$$\vec{V}^{K} = R\vec{V}^{\mathcal{L}} \tag{1.3.8}$$

The resistance between the two nodes m and n are now

$$R^{K}_{mn} = R\frac{|\vec{V}^{\mathcal{L}}_{m} - \vec{V}^{\mathcal{L}}_{n}|}{i_0} \tag{1.3.9}$$

proving that the resistance between two nodes in a network of identical resistors depends linearly on their resistance assuming that current flow does not alter course.

Effect of Nanowire Resistance on Network Conductance

The wire resistivity and cross sectional area are unique to the MNR and so a comparison with JDA cannot be performed for these parameters. Their effect on R_s was determined by applying the MNR model to the NWN pictured in Figure 1.2 with $R_j = 11\Omega$. Figure 1.4(a) shows the effect of changing the resistivity on the sheet resistance. R_s clearly increases in a linear fashion with respect to increasing resistivity which can be attributed to the linear dependence of the resistance of wire segments on the resistivity thus shifting R_0 in the linear formula for R_s given in equation 1.3.2.

Figure 1.4(b) Shows the effect of increasing wire diameter (D) on the sheet resistance of a network. The sheet resistance decreases as a power law relationship, $R_s = cD^{-2} + aR_j$, which is as expected as the nanowire resistance depends on the wire diameter in this way. This power-law relationship is clearly evident in the inset plot which is the same data in log-scale alongside a curve defined by $cD^{-2} + aR_j$ which was included as a guide to the eye. The curve has been offset to the experimental data for ease of viewing.

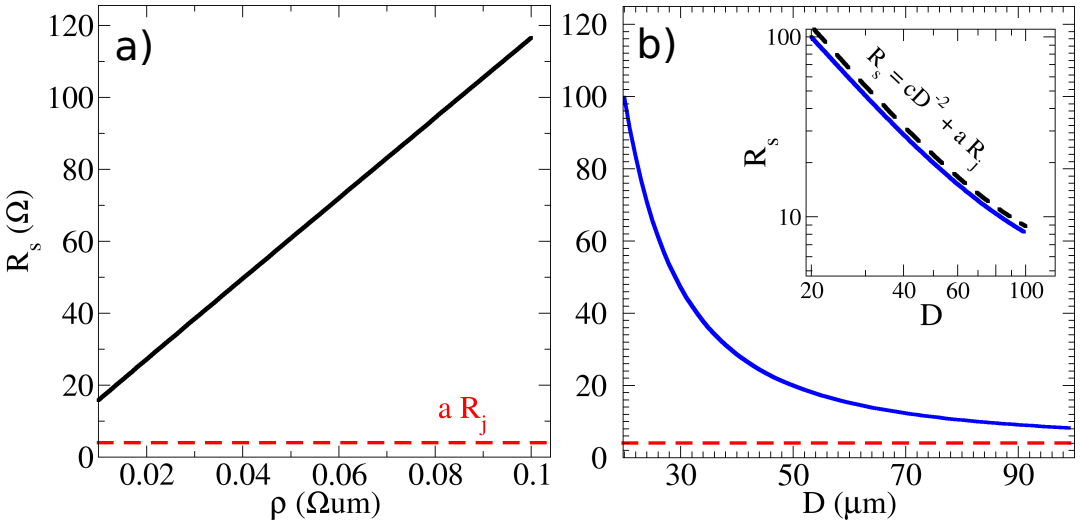

Figure 1.4: a) The dependence of R_s on the resistivity of the nanowires, specific to the network geometry shown in Figure 1.2. R_s depends linearly on the resistivity of the nanowires, the same dependence that the nanowire resistance has on the resistivity. b) The dependence of R_s on the diameter of the nanowires (D), again this relationship follows that of the nanowire resistance on D with a D^{-2} dependence. In the inset the same data is replot in Log-scale in blue. The black dashed line is a guide-to-the-eye curve determined by the equation $cD^{-2} + aR_j$ where c is a constant, note that the equation has been off-set from the data for ease of viewing. Recall $R_s = aR_j + R_0$ and so the sheet resistance tends to a non-zero value determined by the junction resistance for vanishing nanowire resistance. The horizontal dashed line in both plots represents the sheet resistance with no nanowire resistance $R_s = aR_j \approx 4.07\Omega$.

Note that a non-zero junction resistance was used in simulations and so the sheet resistance tends to a non-zero value for vanishing resistivity and infinite wire diameter, $R_s \to aR_j$ as $R_0 \to 0$. This asymptotic sheet resistance is represented by the dashed horizontal line in both plots of Figure 1.4. As the sheet resistance does not tend to a zero value the curves in the log-plot in the inset of Figure 1.4(b) gradually become more horizontal for increasing wire diameter.

If one were to consider a NWN with perfectly conductive junctions ($R_j = 0$) then a symmetry argument similar to that used to describe the linear dependence of R_s on R_j can be used to describe the relationships $R_0 \propto \rho D^{-2}$. An important note should be raised about these symmetry arguments however, they assume that current flow does not redistribute through the network as alterations occur in the

network. It is not inconceivable that in the MNR that an increase in junction or nanowire resistances could cause the current flow to alter course thus causing a shift in the sheet resistance that does not follow the existing linear relationship.

IMPACT OF GEOMETRIC PARAMETERS ON NANOWIRE NETWORK RESISTANCE

[1] The geometric parameters that are common to both the JDA and MNR models are the wire density and wire lengths. Altering either of these parameters results in a fundamental change in the in the connectivity profile. This change is best illustrated by the expression for the junction density derived in chapter 2, $n_j = aL^2 n_w^2$ as it is the junctions that determine the connectivity profile. Recall from the definitions of the JDA and MNR that the junctions are a source of resistance and determine the graphical representations of the NWN.

The geometric parameters have on the connectivity profile is also described by Percolation theory. As discussed in chapter 2, Percolation theory can be used to determine quantities such as the critical wire density below which a conductive path does not form between electrodes. This is described using the equation

$$(n_w)_c = 5.63726 L^{-2} \tag{1.4.1}$$

This equation can be furthered to calculate a critical wire length for a given wire density by simply setting $L \to L_c$ and $(n_w)_c \to n_w$ in equation 1.4.1. Equation 1.4.1 link the wire density and length at the point of criticality and shows how the geometric parameters alter fundamental aspects of the network.

In this section the effect of wire lengths and densities on the network conductance will be explored. As the connectivity profile is altered in a random manner with

1 I may add this section to an appendix or completely remove is as it is not original work. It is here for completeness and referenced in EMT chapter.

a change in either parameter, ensembles of simulations are required. The relationship between sheet resistance and the geometric parameters are then determined through the average of the simulation ensemble.

The effect of wire density on the average R_s calculated in JDA (blue) and MNR (red) for a number of NWNs is displayed in Figure 1.5(a). Other parameters were set to values measured for Ag/PVP core shell nanowires[19] that were used in the previous section; $L = 6.7\mu m$, $R_j = 11\Omega$, $D = 50nm$, and $\rho = 22.6n\Omega m$. Twenty simulations were performed for a given wire density in order to obtain an accurate calculation of the average R_s and the associated confidence interval.

From Figure 1.5(a) the MNR model has a higher sheet resistance for the JDA model at the same densities. This is unsurprising due to the inclusion of nanowire resistance for the MNR and the junction resistances being the same in both models. There is large uncertainty for the average R_s for simulations at lower densities due to being close to the critical density of $(n_w)_c = 0.11 NW/\mu m$ according to equation 1.4.1. A sparse network is susceptible to the stochastic spatial effects of the network and the large uncertainty in the sheet resistance is a manifestation of this randomness. The general decreasing trend of the sheet resistance with increasing nanowire density is a result of additional pathways developing across the network.

According to percolation theory, the sheet conductance Γ_s of a random stick network scales as a power law with the stick density:

$$\Gamma_s \propto (n_w - (n_w)_c)^{-\beta} \tag{1.4.2}$$

Where $(n_w)_c$ is the critical wire density. This scaling law has been well documented in simulations[5,7,14] and has been used to understand the resistive properties of carbon nanotube and metallic nanowire networks[2,20]. Figure 1.5(b) recasts the data from panel (a) in a log-scale plot but alters the horizontal axis to $(n_w - (n_w)_c)$ for comparison with the power law in Equation 1.4.2. Both MNR and JDA have a power law response to the increase in wire density that is easily identifiable in this plot and were fit to both curves. The two models were found to have

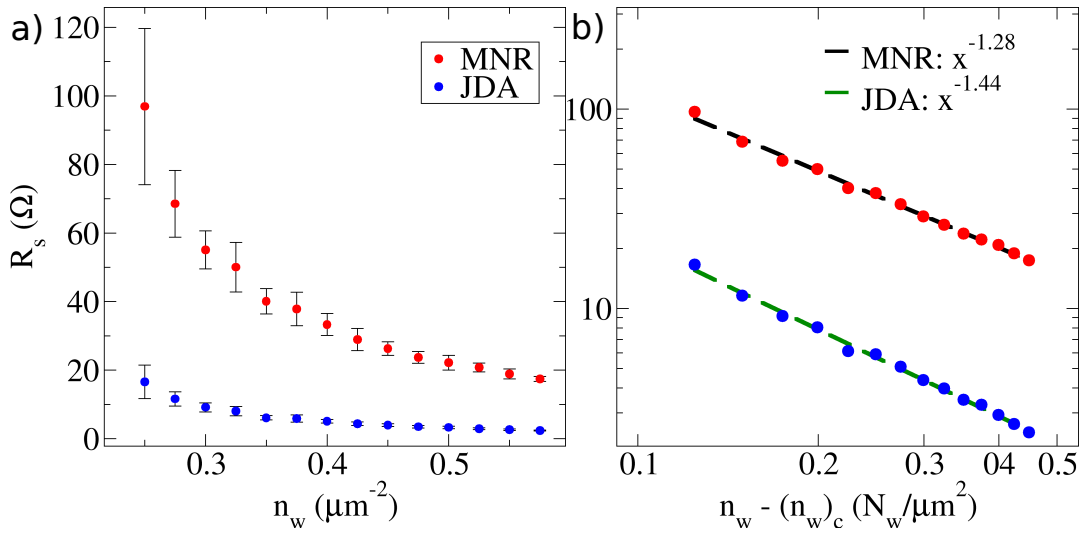

Figure 1.5: (a) The effect of changing wire density n_w on sheet resistance R_s for networks of size $20\mu m \times 20\mu m$ and wires of length $7\mu m$. The wire resistivity, cross sectional area and junction resistance are those measured typical for Ag PVP core shell nanowires. 20 random networks were simulated for each wire density in both MNR and JDA and the average sheet resistance and 95% confidence interval for each wire density was calculated and plot. (b) Sheet resistance versus the parameter $(n_w - (n_w)_c)$ for comparison with equation 1.4.2. Here the two scaling regimes between R_s and n_w is evident for both models. Power-laws were fit to both models and are shown as dotted lines. For the MNR model the scaling exponent according to regression analysis is $\beta_{MNR} \approx 1.28$ and the fitted curve is shown as the black dashed line. The JDA line has an exponent $\beta_{JDA} \approx 1.44$ and is shown as the green dashed line.

differing exponents in their power law fits, $\beta_{MNR} \approx -1.28$ (black dashed line) and $\beta_{JDA} \approx -1.44$ (green dashed line).

These differing exponents are in line with those seen in Monte Carlo simulations that have been reported in the literature. Li and Zhang showed that the scaling exponent depends on the ratio of junction resistance to nanowire resistance (R_{in}). By fitting the Error function to Monte Carlo simulations they found the relationship between the scaling exponent and $x = \log_{10}(R_j/R_{in})$ was

$$\beta = \beta_0 + C\ erf(x) \tag{1.4.3}$$

where $t_0 = 1.314 \pm 0.002$ and $C = 0.108 \pm 0.003$ where the fitting parameters. In the limit of vanishing nanowire resistance, i.e. the JDA model, the exponent is $\beta_{jda} \approx 1.422$. For the MNR model, the resistance of a nanowire of length $6.7\mu m$ and with the resistivity and cross sectional area outlined above is $\approx 77\Omega$ making $\beta_{MNR} = \beta_0 + C\ erf(\log_{10}(11/77)) \approx 1.23$. These exponents are very close to those found in Figure 1.5 and further illustrate the importance of including nanowire resistance in calculations of the sheet resistance. Figure 1.6(a) presents the effect of altering the wire length on the sheet resistance, while keeping wire density fixed to 0.4 μm^{-2} in a NWN of size $20\mu m \times 20\mu m$. Other parameters are fixed to those typical for Ag-PVP nanowires given above. The results of Monte Carlo simulations for both MNR (red data points) and JDA (blue data points) models are presented. The increasing wire length causes the average sheet resistance to increase for both models due to the increase in network connectivity. Also plot is the 95% Confidence interval for the simulations which decrease with wire length. The decrease in variability on the sheet resistance can be understood as the network moving away from the critical length, $(L)_c \approx 3.75\mu m$ according to equation 1.4.1. The MNR model consistently has a higher sheet resistance than the JDA model due to the inclusion of nanowire resistance will make the network more resistive.

Motivated by the scaling between junction conductance and wire density, the scaling between the conductance and the parameter $L - L_c$ was plot in log-scale in Figure 1.6(b). A power-law trend between Sheet resistance and length is clear, and the equation $R_s \propto (L - L_c)^\gamma$ for both models is fit to data. Regression analysis determined that the exponents for the power law scaling was $\gamma_{MNR} \approx 1.03$ and $\gamma_{MNR} \approx 1.45$. Similar to its effect on the scaling exponents for wire density, the inclusion of nanowire resistance drastically alters the exponents.

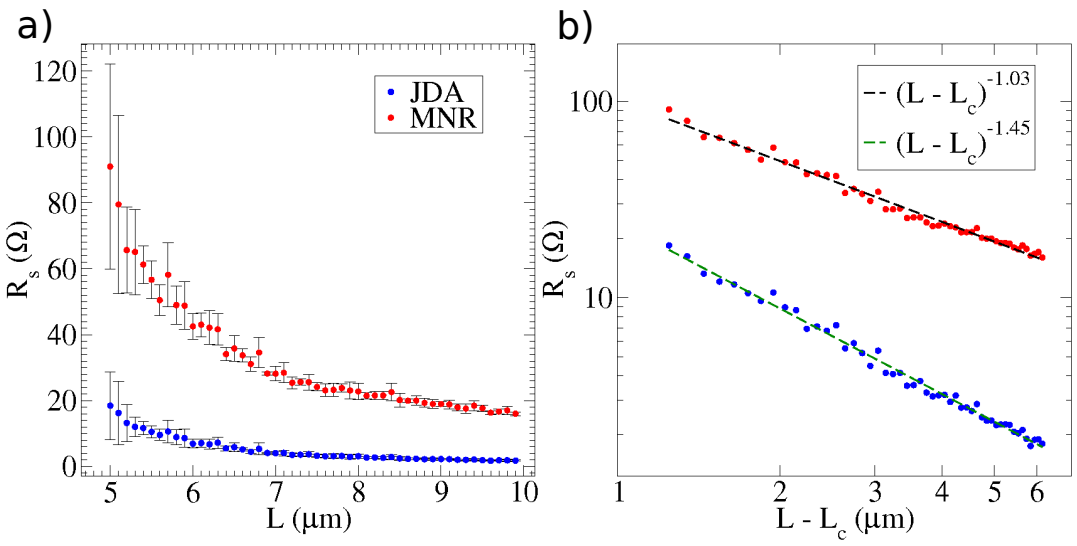

Figure 1.6: (a) The average effect of increasing wire lengths (L) on the sheet resistance (R_s) for networks with a wire density of 0.4 μm^{-2} and of size 20μm $\times$ 20μm in both MNR and JDA models. The wire resistivity, cross sectional area and junction resistance are set to values measured for typical Ag PVP core shell nanowires with $\rho = 22.6 n\Omega m$, D = 50nm, and $R_j = 11\Omega$[19].The average sheet resistance of 10 nanowire networks with a given wire length is calculated for the MNR (red) and JDA (blue) and the 95% confidence interval also shown. (b) The same data as that in Figure (a) recast into log-scale. Here the two scaling regimes between R_s and L is evident for both models. Power-laws were fit to the shorter lengths for both models and are shown as dotted lines. For the MNR model the scaling exponent according to regression is $\gamma_{MNR} \approx 1.03$ and the fitted curve is shown as the black dashed line. The JDA line has an exponent $\gamma_{JDA} \approx 1.45$ and is shown as the green dashed line.

NETWORK GEOMETRY CAPTURE FOR ACCURATE COMPARISON BETWEEN SIMULATION AND EXPERIMENT

A key problem in comparing experimental measurements with computational results is the need to generate an accurate average from simulations. A large number of laborious simulations are required for a meaningful benchmark to compare to and even then a physical sample could have resistances in the extreme tails of ex-

pected outcomes, particularly for low junction density networks. To combat the need for multiple simulations and to allow a more direct comparison with physical samples we developed a method to digitise the geometry of a NWN. This was achieved by opening a scanning-electron-microscope image of a NWN on a digital canvas where the start and end positions of each wire was recorded. The wire is represented as a straight line between these points in the digital version of the NWN. A computational routine to record intersections of the digital wires is performed to determine the junctions and create an approximation of the connectivity profile of the physical NWN. With the positions of each wire and inter-wire junction a 'top-down' 2-dimensional representation of the NWN can be created digitally. Figure 1.8(a) shows a typical Scanning-Electron-Microscope image of a NWN comprising of Ag/PVP core-shell nanowires and Figure 1.8(b) is a representation of the digitised network captured from panel (a).

As eluded to in the previous paragraph, the digital version of the network is an approximation and not a fully accurate representation of the NWN. From the top-down view of the scannin-electron-microscope image it is impossible to tell if an overlap of wires results in physical contact between them, particularly in areas of high wire density where a wire may become suspended above another wire giving the appearance of a junction but in reality there is none. Also the digitisation method approximates every wire as straight lines, wires with significant curvature are not properly represented in the digital network. Finally as the wire positions are determined by eye there is the possibility that some wire positions will not be fully accurate or even not registered.

The sheet resistance of the physical NWN pictured in Figure 1.8(a) was measured experimentally as approximately 42.9Ω. By analysing the dependence of R_s on R_j for both MNR and JDA simulations for the digitised network one can identify a characteristic junction resistance that will lead to the observed experimental sheet resistance. Each junction in the digitised NWN was assigned a resistance R_j and wires in the MNR assigned the measured resistivity ($\rho = 22.6 n\Omega m$) and diameter

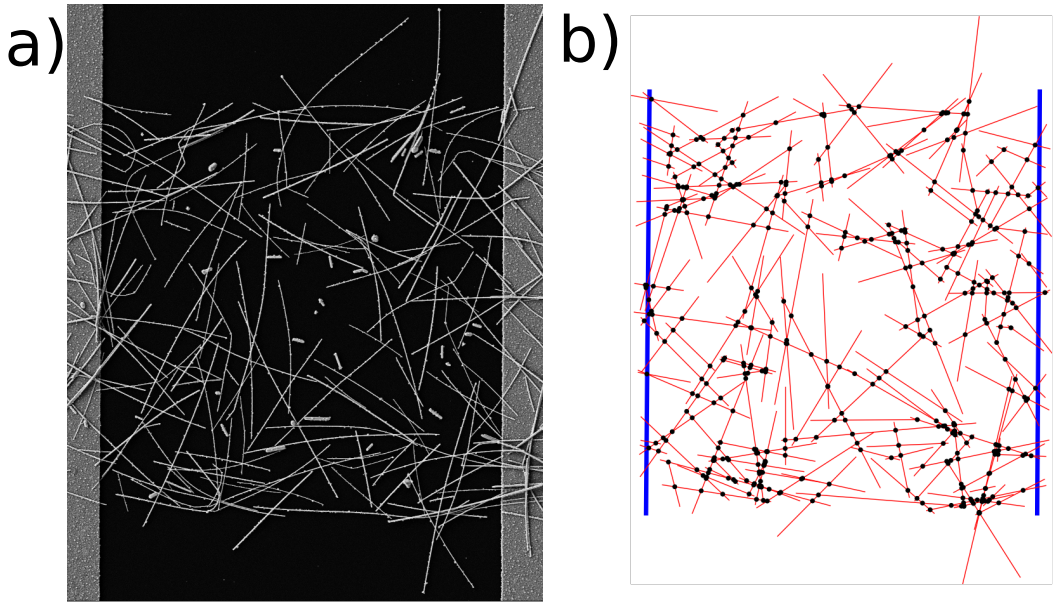

Figure 1.7: a) An scanning-electron-microscope of a physical nanowire network that is roughly $20\mu m \times 20\mu m$ in size. nanowires can be seen against the black background with electrodes seen to the left and right of the network. b) A representation of the digitised NWN that was depicted in a). Black dots represent inter-nanowire junctions and the blue vertical lines represent the electrodes.Note: Quality needs to be improved

($D = 50nm$) for Ag/PVP nanowires. R_s was calculated for both models and this process was repeated for many values of R_j, the results of which are plot in Figure 1.8. Also shown in Figure 1.8 is the experimental sheet resistance R_{exp} and is represented by the horizontal dashed line. Where it intersects with the JDA sheet resistance curve (R_s^{JDA}) and the MNR sheet resistance curve (R_s^{MNR}) provides two characteristic junction resistances, $R_j^{JDA} \approx 96.9\Omega$ and $R_j^{MNR} \approx 52.9\Omega$. The difference between the characteristic junction resistances is sizeable, approximately 44Ω, illustrating the large impact the nanowire resistance has on the sheet resistance.

As seen in Section 1.3 the two resistive curves offer much insight into the behaviour of the network. Recall that the equations for R_s in terms of R_j for both models are

$$R_s^{JDA} = \alpha R_j \tag{1.5.1}$$

$$R_s^{MNR} = \alpha R_j + R_0 \tag{1.5.2}$$

where the fitting parameters are $\alpha \approx 0.443$ and $R_0 \approx 16.2\Omega$ for this sample. Recall that the slope of the line α can be used to understand how current flows through the NWN, either through a few or a large number of paths in the network. In this case $\alpha \approx 0.443$ leading to the conclusion that current flows through many parallel paths, more paths than resistors in the characteristic path between electrodes.

The experimental sheet resistance for 30 electrically annealed samples were measured and the network geometry were digitised. R_s versus R_j curves were generated for each of the digitised network geometries in the same manner as Figure 1.8. The linear equations for R_s outlined in equation 1.5.2 were applied to each digitised network and from it the characteristic junction resistances were obtained as well as the slope α. Figure 1.9(a) displays the characteristic junction resistances obtained from the MNR (red triangles) and the JDA (blue dots) models plot against wire density n_w. There does not appear to be any relationship between R_j and n_w, indeed the only discernible pattern being R_j^{JDA} are consistently lower than R_j^{MNR}. Note that the junction resistances appear in the range $2.28 \leqslant R_j^{MNR} \leqslant 152\Omega$ and R_j^{JDA} in the range $42.35 \leqslant R_j^{MNR} \leqslant 185.91\Omega$. In Figure 1.9(b) the slope α is plot against the wire density and a clear trend is observed between the two. The decrease in α as wire density increases suggests an increasing number of parallel paths between electrodes as the wire density increases as one would expect. [2]

The calculation of the characteristic junction resistance assumes that the resistances in the network are identical which is not the case in reality, however it does provide a illustrative estimate. The resistance of several individual Ag/PVP

2 A separate symbol for characteristic junction resistance?

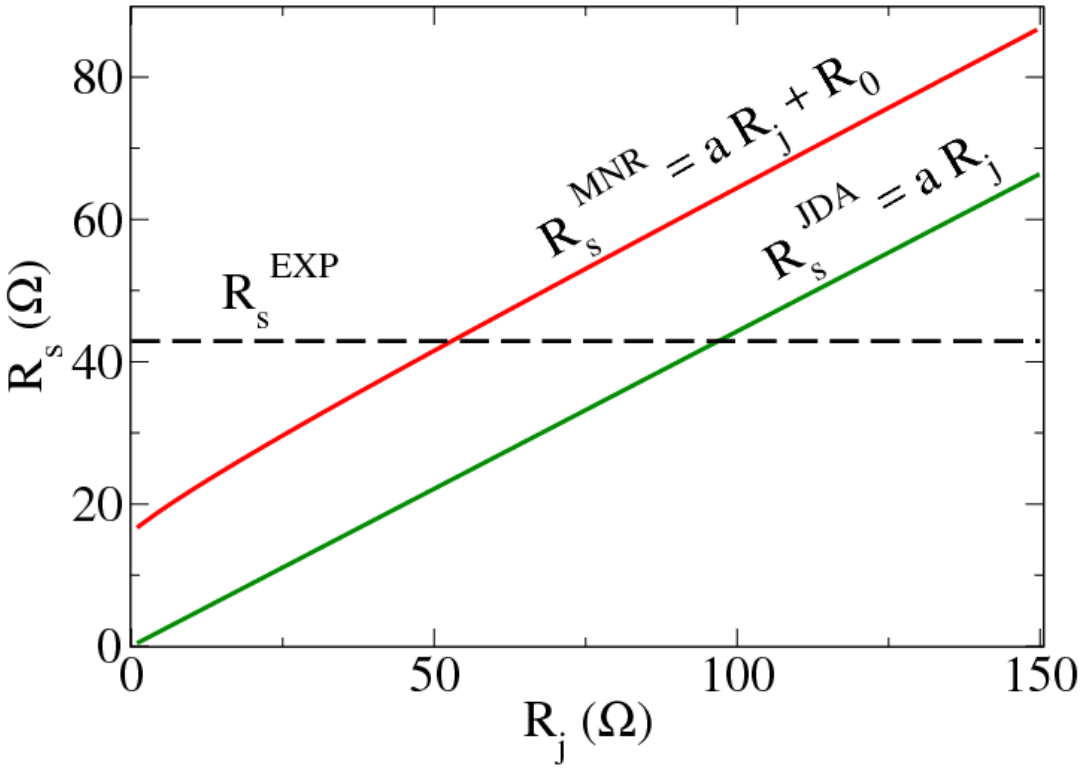

Figure 1.8: The relationship between the sheet resistance of the digitised network (a) in MNR and JDA models wit increasing the junction resistance (R_j). One finds $R_s^{MNR} = aR_j + R_0$ and $R_s^{JDA} = aR_j$ where $a \approx 0.443$ and $R_0 \approx 16.2\Omega$ from regression analysis. The horizontal line represent the sheet resistance that was experimentally measured for this sample, $42.9\Omega/sq$. The value for R_j required for the MNR and JDA to obtain a sheet resistance corresponding to that measured in experiment are identified, $R_j^{MNR} \approx 52.9\Omega$ and $R_j^{JDA} \approx 96.9\Omega$.

nanowire junctions that had been electrically or thermally annealed were measured by Bellew et al, the distribution of recorded resistances are shown in Figure (a). The majority of junctions were found to have resistances less than 70Ω, however there were two junctions whose resistance were very high with values in the range $200 - 300\Omega$. These two measurements represent 6.25% of the measured junction resistances and will be referred to as outliers from here on. There is a clear spike in frequency of junction resistances in the range $10 - 20\Omega$ and the median junction resistance of 11Ω occurs in this bin.Figure (b) is a distribution of the characteristic junction resistances from the MNR model for the experimental samples that were shown in Figure 1.9(b). The characteristic junction resistance is much higher than

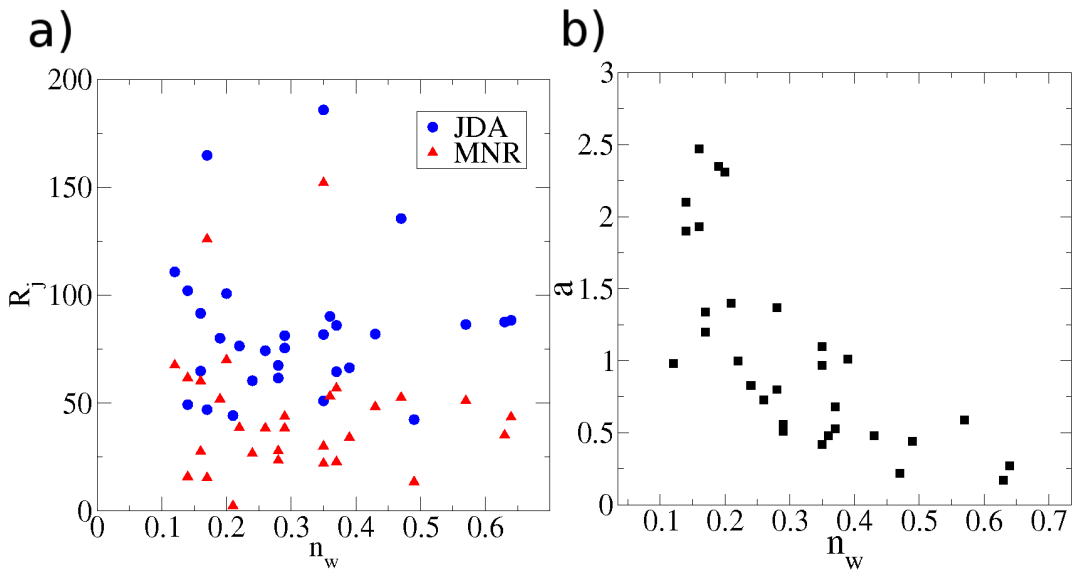

Figure 1.9: (a) The characteristic junction resistances obtained from applying MNR (red triangles) and JDA (blue dots) to 30 experimental NWN samples versus the measured wire density of said samples. No clear relationship is observed between n_w and R_j. (b) The slope coefficient a versus n_w for the 30 experimental samples.

the measured junction resistances shown in Figure 1.10(a), the mean value is 44.9Ω and the median value of 38.4Ω. While it is higher than the measured sheet resistance is does show that the characteristic junction resistance is of the correct order of magnitude of tens of Ohms. The inclusion of nanowire resistance in simulations results in a more accurate characteristic junction resistance, recall from Figure 1.9(a) that the MNR resistances are always less than those found for the JDA.

To minimise a physical network's conductivity an annealing technique is usually applied, in the case of the 30 samples referred to in this thesis this was a gradual electrical stressing[19]. To understand a NWNs maximum potential conductivity the dimensionless optimisation-capacity coefficient (γ) was introduced

$$\gamma = 1 - \frac{R_0}{R_s^{exp}} \tag{1.5.3}$$

γ varies between zero and one, values of γ close to one indicate the conductance of the network can be considerably improved. When γ is nearer to zero the network is

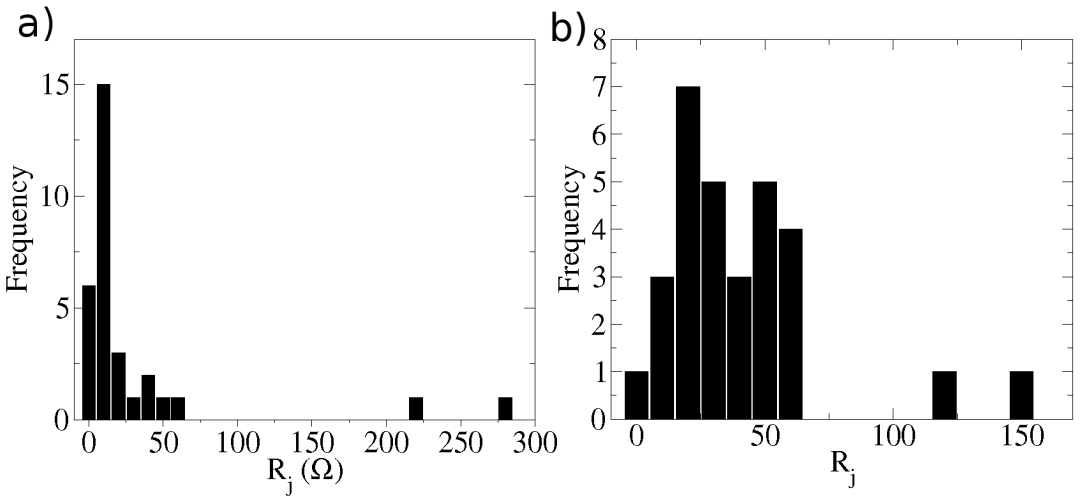

Figure 1.10: (a)Distribution of resistances measured for 32 individual nanowire junctions. There is a clear spike in frequency at the median resistance of 11Ω (b) The distribution of the Characteristic junction resistances that were shown in Figure 1.9(a). The average resistance is 44.9Ω and median value is 38.4Ω, of the same order of magnitude as that measured experimentally. The bin sizes are of size 10Ω for both distributions. put R_j^MNR on axis.

near its optimum conductivity, i.e. the skeletal nanowire resistance R_0, as all of the junctions in the network have been annealed into a perfectly conductive state. This metric provides fabricators of NWNs with an idea of the potential improvement possible in a particular network. Figure 1.11(a) shows a plot of the relationship between wire density and γ which was determined for each of the 30 experimental samples. There does not appear to be a relationship between the two parameters suggesting that the electrical annealing was as successful on a network regardless of the wire density. Figure 1.11(b) plots γ versus the characteristic junction resistance for each sample. A clear relationship exists between R_j and γ, the junction resistance the more room for improvement in the NWN conductance.

The importance of including nanowire resistivity in comparisons between computational simulations and experimental measurements was demonstrated in this section through the MNR model. Not only does the MNR model more actually estimate the resistance of annealed junctions it also identifies the ultimate conductivity of a network, that which is limited by the skeletal nanowire resistance. The

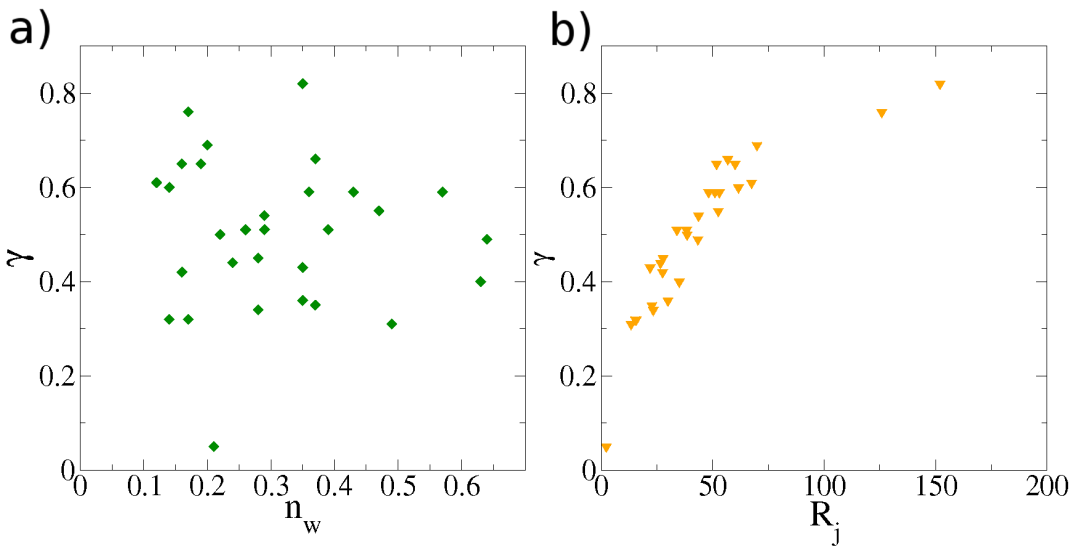

Figure 1.11: a) Wire density (n) versus the Optimisation Capacity Coefficient (γ) for 30 experimental NWN. There is no discernible relationship between the two parameters. b) The Optimisation Capacity Coefficient (γ) versus the MNR characteristic junction resistances for the 30 experimental NWN samples shown in Figure 1.9(a). A clear relationship exists between the two parameters.

simulation results unique to each experimental sample presented in this chapter are numerical and take a great deal of sample processing to obtain. In the following chapter an analytical approximation for the sheet resistance in terms of the fundamental properties are presented which provides a quick and mathematically transparent method to estimate various properties of a network.

CHAPTER CONCLUSION

The importance of including the contribution of nanowire resistance to that of NWNs was highlighted in this chapter. The electrical properties of NWNs can be calculated by mapping the NWN onto a node-voltage lattice, the electrical properties of which can be calculated using Ohm's and Kirchhoff's laws. Two node-voltage mappings were introduced, the Junction Dominated Approach (JDA) and

the Multi-Nodal Representation (MNR). The JDA model assumes that the electrical properties of the network are dominated by the junction resistances and so the nanowire resistances are ignored while the MNR model includes them. The dependence of the sheet resistance in the MNR model on wire resistivity and wire diameter was shown to be $R_s \propto \rho D^{-2}$. A linear relationship between sheet resistance (R_s) and junction resistance (R_j) was shown to hold mathematically and in simulations for JDA models of NWNs such that $R_s^{JDA} = \alpha R_j$. The same linear relationship was shown in simulations of MNR models of NWNs plus a contribution from the nanowire resistance, $R_s^{MNR} = \alpha R_j + R_0$.

The effect of wire lengths and wire densities were also explored in both models. Since these parameters can alter the connectivity of a NWN drastically the need for spatial configurational averaging arose. A large number of simulations altering either the wire density or the wire lengths were performed and the corresponding average sheet resistances were plot for MNR and JDA. Power law relationships between sheet resistance and wire length and density were observed as one would expect from percolation theory. The inclusion of nanowire resistance was shown to alter the value of the exponent in the percolative power laws.

A method to capture the geometrical layout of a physical NWN sample from an scanning-electron-microscope image was presented which allows for simulations on geometries similar to the experimental samples. Thirty samples who's sheet resistance had been measured were digitised and both were used to understand the nature of current flow and junction resistances in a NWN. Linear expressions relating the sheet resistance and junction resistance were found for each sample in MNR and JDA simulations and were used to determine a characteristic junction resistance, the value at which simulated R_s match the experimental R_s. The characteristic junction resistance was found to be lower for MNR model than the JDA model which can be explained with the sizeable impact of nanowire resistance on the network. The distribution of MNR characteristic junction resistances were compared with a distribution of single Ag/PVP junction resistances experimentally

measured by Bellew et al[13]. The simulated characteristic resistances overestimated the measured junction resistances but were of the same order of magnitude of tens of Ohms. Characteristic junction resistances calculated with the MNR model were more accurate than those from the JDA model further highlighting the need for nanowire resistances.

The Ultimate Conductivity of a network was shown to be limited by the contribution of the nanowire resistances. A measure of how much potential for conductivity improvement was introduced, the optimisation capacity coefficient (γ), and was calculated for the experimental samples. There was no direct relationship between γ and wire density suggesting that the electrical annealing process was equally effective for all of the networks. However γ did depend on the characteristic junction resistance, where NWNs with higher resistances had higher values of γ meaning there was much room for improvement. [3]

3 A general note, should plots be made bigger?

BIBLIOGRAPHY.BIB

---

[1] D. Hecht, L. Hu, and G. Grüner, "Conductivity scaling with bundle length and diameter in single walled carbon nanotube networks," *Applied Physics Letters*, vol. 89, no. 13, p. 133112, 2006.

[2] S. M. Bergin, Y.-H. Chen, A. R. Rathmell, P. Charbonneau, Z.-Y. Li, and B. J. Wiley, "The effect of nanowire length and diameter on the properties of transparent, conducting nanowire films," *Nanoscale*, vol. 4, pp. 1996–2004, 2012.

[3] S. Sorel, P. E. Lyons, S. De, J. C. Dickerson, and J. N. Coleman, "The dependence of the optoelectrical properties of silver nanowire networks on nanowire length and diameter," *Nanotechnology*, vol. 23, no. 18, p. 185201, 2012.

[4] J. Hicks, A. Behnam, and A. Ural, "Resistivity in percolation networks of one-dimensional elements with a length distribution," *Physical Review E*, vol. 79, no. 1, p. 012102, 2009.

[5] G. E. Pike and C. H. Seager, "Percolation and conductivity: A computer study. i," *Phys. Rev. B*, vol. 10, pp. 1421–1434, Aug 1974.

[6] R. M. Mutiso, M. Sherrott, A. Rathmell, B. Wiley, and K. Winey, "Integrating simulations and experiments to predict sheet resistance and optical transmittance in nanowire films for transparent conductors," *ACS Nano*, vol. 7, no. 9, pp. 7654–7663, 2013.

[7] M. Žeželj and I. Stanković, "From percolating to dense random stick networks: Conductivity model investigation," *Phys. Rev. B*, vol. 86, p. 134202, Oct 2012.

[8] I. Balberg, N. Binenbaum, and C. Anderson, "Critical behavior of the two-dimensional sticks system," *Physical Review Letters*, vol. 51, no. 18, p. 1605, 1983.

[9] J. A. Fairfield, C. Ritter, A. T. Bellew, E. K. McCarthy, M. S. Ferreira, and J. J. Boland, "Effective electrode length enhances electrical activation of nanowire networks: Experiment and simulation," *ACS Nano*, vol. 8, no. 9, pp. 9542–9549, 2014. PMID: 25153920.

[10] S. Kirkpatrick, "Percolation and conduction," *Rev. Mod. Phys.*, vol. 45, p. 574, 1973.

[11] C. Pozrikidis, *An Intrduction to Grids, Graphs and Networks*. Oxford University Press, 2014.

[12] P. N. Nirmalraj, P. E. Lyons, S. De, J. N. Coleman, and J. J. Boland, "Electrical connectivity in single-walled carbon nanotube networks," *Nano letters*, vol. 9, no. 11, pp. 3890–3895, 2009.

[13] A. T. Bellew, H. G. Manning, C. G. Rocha, M. S. Ferreira, and J. J. Boland, "Resistance of single ag nanowire junctions and their role in the conductivity of nanowire networks," *ACS Nano*, vol. 9, p. 11422, 2015.

[14] J. Li and S. Zhang, "Finite-size scaling in stick percolation," *Phys. Rev. E*, vol. 80, p. 040104, Oct 2009.

[15] A. R. Madaria, A. Kumar, F. N. Ishikawa, and C. Zhou, "Uniform, highly conductive, and patterned transparent films of a percolating silver nanowire network on rigid and flexible substrates using a dry transfer technique," *Nano Research*, vol. 3, no. 8, pp. 564–573, 2010.

[16] S. De, T. M. Higgins, P. E. Lyons, E. M. Doherty, P. N. Nirmalraj, W. J. Blau, J. J. Boland, and J. N. Coleman, "Silver nanowire networks as flexible, transparent, conducting films: Extremely high dc to optical conductivity ratios," *ACS Nano*, vol. 3, no. 7, pp. 1767–1774, 2009.

[17] S. De and J. N. Coleman, "The effects of percolation in nanostructured transparent conductors," *MRS Bulletin*, vol. 36, pp. 774–781, 10 2011.

[18] C. O'Callaghan, C. G. da Rocha, H. G. Manning, J. J. Boland, and M. S. Ferreira, "Effective medium theory for the conductivity of disordered metallic nanowire networks," *Physical Chemistry Chemical Physics*, vol. 18, no. 39, pp. 27564–27571, 2016.

[19] C. G. Rocha, H. G. Manning, C. O'Callaghan, C. Ritter, A. T. Bellew, J. J. Boland, and M. S. Ferreira, "Ultimate conductivity performance in metallic nanowire networks," *Nanoscale*, vol. 7, p. 13011, 2015.

[20] L. Hu, D. S. Hecht, and G. GrÃŒner, "Percolation in transparent and conducting carbon nanotube networks," *Nano Letters*, vol. 4, no. 12, pp. 2513–2517, 2004.